AD_____

AWARD NUMBER DAMD17-95-C-5038

TITLE: Perimetric Mapping of Hyperacuity: Effects of Retinal Laser Scars

PRINCIPAL INVESTIGATOR: Elmar T. Schmeisser, Ph.D.

CONTRACTING ORGANIZATION: University of Kentucky
Lexington, Kentucky 40506-0056

REPORT DATE: June 1997

TYPE OF REPORT: Final

PREPARED FOR: Commander
U.S. Army Medical Research and Materiel Command
Fort Detrick, Maryland 21702-5012

DISTRIBUTION STATEMENT: Approved for public release;
distribution unlimited

REPORT DOCUMENTATION PAGE

Form Approved
OMB No. 0704-0188

1. AGENCY USE ONLY *(Leave blank)*	2. REPORT DATE	3. REPORT TYPE AND DATES COVERED
	June 1997	Final (25 May 95 - 24 May 97)

4. TITLE AND SUBTITLE
Perimetric Mapping of Hyperacuity: Effects of Retinal Laser Scars

5. FUNDING NUMBERS
DAMD17-95-C-5038

6. AUTHOR(S)
Elmar T. Schmeisser, Ph.D.

7. PERFORMING ORGANIZATION NAME(S) AND ADDRESS(ES)
University of Kentucky
Lexington, Kentucky 40506-0056

8. PERFORMING ORGANIZATION REPORT NUMBER

9. SPONSORING / MONITORING AGENCY NAME(S) AND ADDRESS(ES)
U. S. Army Medical Research and Materiel Command
Fort Detrick, Maryland 21702-5012

10. SPONSORING / MONITORING AGENCY REPORT NUMBER

11. SUPPLEMENTARY NOTES

12a. DISTRIBUTION / AVAILABILITY STATEMENT
Approved for public release; distribution unlimited

12b. DISTRIBUTION CODE

13. ABSTRACT *(Maximum 200 words)*

The effects of specific graded retinal laser lesions on both vernier acuity and local luminance perimetry were measured by electrophysiological means. Seven Cynomolgus fasciculata received minimal spot laser exposures 6 years previously from a q-switched Nd-YAG laser (1064 nm) at energies up to and including contained subretinal hemorrhages in both the parafovea and the fovea. High contrast vernier acuity targets were presented at high luminance levels to anesthetized primates. Visual evoked potentials were recorded by conventional means. A significant decrease of the pattern response signal/noise, and a relative loss of vernier signal was seen in the lesioned eyes. Animals with the more severe lesions have degraded small pattern responses and no recordable vernier response. Lesser apparent losses produced less effect. Finally, a map of each retina was produced by flickering small patches on the stimulus display and recording the retinal signal. The multifocal (perimetric) electroretinogram was recorded from specialized contact lenses. Relative response losses of no more than 25% were seen at sites corresponding to the more severe foveal lesions.

14. SUBJECT TERMS
Acuity, Aiming, ERG, Eye, Laser, Lesion, Primates, Retina, Healing, Perimetry, VEP, Wolfe grade

15. NUMBER OF PAGES
45

16. PRICE CODE

17. SECURITY CLASSIFICATION OF REPORT	18. SECURITY CLASSIFICATION OF THIS PAGE	19. SECURITY CLASSIFICATION OF ABSTRACT	20. LIMITATION OF ABSTRACT
Unclassified	Unclassified	Unclassified	Unlimited

FOREWORD

Opinions, interpretations, conclusions and recommendations are those of the author and are not necessarily endorsed by the U.S. Army.

____ Where copyrighted material is quoted, permission has been obtained to use such material.

____ Where material from documents designated for limited distribution is quoted, permission has been obtained to use the material.

X Citations of commercial organizations and trade names in this report do not constitute an official Department of Army endorsement or approval of the products or services of these organizations.

X In conducting research using animals, the investigator(s) adhered to the "Guide for the Care and Use of Laboratory Animals," prepared by the Committee on Care and use of Laboratory Animals of the Institute of Laboratory Resources, national Research Council (NIH Publication No. 86-23, Revised 1985).

____ For the protection of human subjects, the investigator(s) adhered to policies of applicable Federal Law 45 CFR 46.

____ In conducting research utilizing recombinant DNA technology, the investigator(s) adhered to current guidelines promulgated by the National Institutes of Health.

____ In the conduct of research utilizing recombinant DNA, the investigator(s) adhered to the NIH Guidelines for Research Involving Recombinant DNA Molecules.

____ In the conduct of research involving hazardous organisms, the investigator(s) adhered to the CDC-NIH Guide for Biosafety in Microbiological and Biomedical Laboratories.

PI - Signature 4/16/97 Date

Perimetric Mapping of Hyperacuity:

Effects of retinal laser scars --

Final Report

Elmar T. Schmeisser, Ph.D.

Table of Contents

1. INTRODUCTION

Vision, and visual compromise due to retinal burns caused by laser exposure, has been evaluated and measured in many different ways. Visual field effects, changes in grating acuity, gray scale contrast sensitivity and chromatic sensitivity have all been measured in the attempt to quantitate a very complex sense system. Previous studies both by this author and many others have examined the effect of laser exposures on the electrophysiological responses of the retina.[1-17] In some cases, the interest was in very acute changes, while in many others, only longer term studies were possible. Long term studies on the functional recovery of the retina subjected to discrete laser lesions have not been completed, nor are most techniques available suitable for noninvasive examination of small disjunct retinal areas.

This experiment specifically investigates the ability of the visual system to make localization judgments, i.e. vernier or hyperacuity, as opposed to pattern resolution judgments, e.g. grating or letter acuities.[18] The ability of an observer to correctly judge the offset of 2 dots or line elements is quite resistant to optical degradation and is significantly different in its response to pathology.[19-20] Additionally, this ability is critical to aiming and tracking tasks common to many activities, including simply driving down the road between the lines and parking a vehicle. Visual evoked potential correlates of hyperacuity have been obtained in humans.[21-23] These studies show that

the hyperacuity VEP in humans scales linearly with log offset and thus can permit estimation of the psychophysical hyperacuity threshold by extrapolation to signal amplitude extinction. However, vernier acuity falls off with retinal eccentricity even faster than resolution acuity or contrast sensitivity.[24]

Further, over the past few years, an innovative experimental technique has been introduced that may help to address this problem: multi-input electroretinography.[25,26] This method uses a tiled stimulus display in which each hexagonal tile is flickered independently such that the overall averaged luminance change is zero and each tile has a unique temporal signature (the m-sequence technique). The ERG is recorded to this multiple stimulus from a single recording electrode and then cross-correlated to each tile's individual signature. This results in a topographic or perimetric map of the retinal response which seems to correlate with ganglion cell density across the retina. A previous attempt by the author to use this technique was unable to produce sufficient signal/noise enhancement to provide reliable data.[27] These problems have now been solved.

The animals used in this study have had graded laser lesions placed 6 years previously by the native collimated beam from a pulsed Nd-YAG laser emitting 1062 nm light without expansion or focusing by any lens system other than that of the eye itself. Placement and severity of these lesions was governed by attempts to produce "Wolfe grade" equivalent effects[4] with single Q-switched exposures. Four lesions had been placed in the right

eye of each animal, the left eye serving as a normalizing control with no laser exposures. The exposure energy (and thus lesion type) was counterbalanced across both locations and animals for severity and only four exposures were made in the right eye of each animal. The acute effects of these lesions on acuity as measured by the sweep VEP technique have been previously reported.[17]

Summarizing the 7 animals in this experiment, at the foveal site there are 2 animals which were labeled with no visible change at the time of exposure, 2 with a "minimal visible lesion" (MVL, or Wolfe Grade $1B^4$), 2 with "white dot" lesions (retinal blanching, grade IIB) and 3 with "red dot" lesions (contained retinal hemorrhage, grade IIIB). At the parafoveal locations, there are 11 sites with no visible change at the time of exposure, 4 sites with MVL (IA), 6 sites with a white dot lesion (IIA), and 4 sites with a red dot lesion (IIIA). Their current appearance varies, in some cases drastically, from the grading at the time, ranging from some "red dot" lesions almost vanishing to now relatively prominent "minimally visible" lesions (appendix A).

Since as noted above, the VEP falls off with eccentricity due to both cortical magnification and to the topographic mapping of the visual field on the cortex, the signal to noise ratio of the VEP will fall off drastically in any attempt to record a response from the periphery with noninvasive methods.[23] Accordingly, this report is limited to the examination of the

vernier VEP responses when the stimulus is placed on the foveal area itself. The consideration whether isolated peripheral lesions have any additional effect to that of the foveal exposure must await a further study with different animals, although some indications are presented here. Finally, as noted above, in order to identify the amount of absolute functional decrement, the retinal areas were mapped with ERG perimetry and correlated with fluorescein angiographic images.

2. METHODS

Detailed methods, dose regimes, rationales and procedures are presented in appendices B & C for the cortical and retinal recordings, respectively; a summary only is given here. All procedures were preapproved and annually reviewed by the University of Kentucky IACUC, and followed NIH and ARVO guidelines. Anesthetized animals were maintained and monitored at physiological conditions throughout the recording and photographic sessions, and were housed in AAALAC approved facilities between sessions. Visual evoked potentials (VEPs) and multifocal electroretinograms (ERGs) were recorded by conventional means. VEPs were recorded to contrast reversing checkerboards and to a repeatedly occuring lateral offset and realignment of a vernier pattern. Multifocal ERGs were recorded to a 16 degree diameter pattern of packed equal area hexagons centered on the fovea. Ocular photography included both color fundus pictures of each exposed eye, and an associated fluorescein angiogram (FA). For the FA sessions, muscular relaxation via pancuronium bromide was

not used, and only the ketamine/acepromazine IM sedation and pentobarbital IV anesthesia at the standard doses was employed. Depending on the animal's size, between 0.25 and 0.5 ml of 10% sodium fluorescite was injected IV for the imaging study. As noted above, copies of each experimental eye's fundus photograph and late phase FA image are in appendix A.

Over the duration of this project, of the 9 animals originally exposed as part of a previous contract investigating acute effects of laser esposure, one was terminated on the veterinarian's recommendation due to advanced systemic illness soon after the initial exposures, and was not available for this study. A second animal developed untreatable diabetes and concurrent cataracts, and was also terminated before useful data could be obtained. The data in this report and the appendices are based on the remaining seven animals. Arrangements have been made for histological recovery and characterization of the ocular tissues from the seven animals covered in this report.

3. RESULTS

Detail results with illustrative figures for each phase of the study are given in appendices B (for sections 3.1 & 3.2 below) & C (for section 3.3 below). A summary of the main findings is given here.

3.1 VEPs to checkerboard patterns: The signal to noise ratios derived from the power spectral densities of the steady state pattern VEPs showed that as a class, the more severely exposed

eyes have lower log(signal/noise) than the normal eyes (P=0.036); however overall response power itself was not significantly different as a function of either eye, or exposure class. There was a tendency towards more severe effects with more severe lesions, but this did not attain significance (p=0.27). Spatial frequency was as expected a significant factor (P=0.005) with the lowest spatial frequency demonstrating a stronger (larger) response than the smaller patterns, i.e. a tuning curve.

3.2 VEPs to vernier offsets: With large offsets, the response decreases in the lesioned eye while remaining recordable from the control eye. Comparison of the maximum responses (measured via time shifted cross-correlations against a normal summed template response) between exposure classes (minimal vs white or red lesions) in the experimental eye demonstrated a tendency towards more severe losses with the more severe lesion, but the effect did not attain significance (p=0.152). In contrast, examination of the correlation results with no offset in time showed an interaction effect between lesion class and eye (p=0.041). Looking at only the exposed eye and analyzing for the effect of lesion class across all vernier offsets, the more severe lesion was significantly more effective in dropping the response (p=0.033). Finally, there is a tendency for the interocular correlation to drop with the more severe lesions, but this did not attain significance in this small sample (p=0.13).

A related finding was that off-axis burns (approx. 5 degree eccentricity) did not seem to affect central vernier acuity in

these particular long term animals, e.g. one animal with an apparent MVL in the fovea but with white and red dot lesions in periphery has vernier VEP responses that were not significantly different between the control and exposed eye.

3.3 ERGs to topographic mapping stimuli: All ERG maps of eyes with obvious discrete lesions showed remarkably small circumscribed areas of somewhat reduced response, even in those retinas noted as having "red dot" lesions at the time of placement. Visually, the 3-dimensional maps appeared to be "volcano" shaped rather than showing a more or less smooth "hill of vision". The caldera of this volcano ranged from about a 10% drop in response compared to the areas immediately adjacent to approximately 25% in one eye with a bridging scar between the foveal site and the superior site. Most of the maps also showed some edge artefacts (loss of signal), especially in the inferior field that may have been due to partial occlusion of the upper edge of the pupil by the central recording element in the contact lens. As a result, mapping of the peripheral lesions may have to be done explicitly. Lesions of the MVL type were not clearly apparent, nor were all the white dot type lesions.

4. DISCUSSION

The decrease in signal to noise ratio in the relatively large field pattern VEPs without a concomitant loss of absolute response power in intriguing. Does an abnormal fovea actually increase the visual system's noise as opposed to simply removing

its contribution to the response? This type of masking or interference may have functional consequences that extends beyond the apparent lesion diameter, and would need to be separately considered. On the other hand, the data presented here does not support the inverse idea, viz. that damaged peripheral retina has a significant ability to affect foveal function as measured by pattern VEP.

The comparison between the responses to checkerboard stimuli and vernier stimuli of a comparable size indicates that the vernier response is probably even more sensitive to retinal disruption, a finding in opposition to that noted with optical compromise. This might be expected, since the pattern VEP responses were obtained with stimuli that covered normal as well as abnormal retina, but the localized vernier stimuli may not have impinged on unexposed retina, and in the case of the most severe lesions, may not extend outside a presumed local scotoma. Other data exists that implicates retinal ganglion cells as being the limiting factor in vernier resolution.[28] While this data was obtained in cats rather than primates, if the physiological mechanism holds across species, the apparent damage to vernier acuity with the current laser lesions implies that the cortex may not be able to compensate for these retinal signal losses, unlike the image filling in or illusory border completion that can occur with more extended patterns.[29] In summary, the vernier VEP analyses imply that for any offset size, including those well above normal vernier threshold, 1) there tends to be a drop due

to any foveal exposure, and 2) this drop appears to be more severe with greater lesions.

It should be reiterated that not all animals produced recordable vernier VEPs with this protocol, even from their normal eyes. This tended especially to be the case for the larger (male) animals and may be an artefact of their greater skull thickness and head musculature combined with the small size of the signal when recorded by surface (either subcutaneous needle or scalp cup) EEG electrodes. In order to improve this situation, implantation of chronic electrodes to record from at least the dural surface if not transcortically probably would be required.[14] Finally, an exhaustive perilesional mapping protocol in order to maximize any vernier signal by placing it just outside of a (presumed) lesion scotoma was not undertaken. Behavioral studies which would allow the animal to adopt individual compensatory strategies (such as off axis viewing with alternate preferred retinal loci) might be more appropriate to determine the final functional consequences of discrete retinal lesions such as those in this study.

In contrast to the previous report of results with these animals using the ERG mapping technique,[27] further work has shown that there are three prerequisites for successful recording: 1) good oculostasis, insured by pentobarbital and pancuronium medication, 2) a well fitted nonglaring bipolar ERG contact lens with the correct contact lens curvature as well as acceptable electrical and optical properties, and 3) refraction by streak

retinoscopy over the contact lens to correct both for the stimulus distance and the animal's own refractive error, if any, as well as for the lens induced changes.

It should be noted that each map took 8 minutes to acquire, and several maps were averaged to obtain the data. Some eye drift was bound to occur since the recordings were not made under optically stabilized conditions, nor under infrared visual monitoring. As a result, the response profiles may be somewhat shallower and the actual limits of the response losses less distinct than may be in fact the case. However, this drift could only have been on the order of a few degrees since the alignment was checked before and after the series of runs, and in most cases seemed stable to visual inspection. Nevertheless, that there is as much signal as was seen in these cases implies that these focal lesions do not have a wide spread effect on the entire retina, nor that all luminance processing close by, if not at, the lesions site is destroyed. Whether this retention of signal generating ability is due to the healing process, e.g. photoreceptor migration into the lesion site, must await histological recovery of the tissue.

A final point concerns the possibility of deeper functional deficits in the maps when the visual system is queried with more demanding stimuli, e.g. patterns. This is best done electrophysiologically with the visual evoked potential (VEP). The few maps were obtained that seemed to indicate that the VEP can demonstrate lesions that are not apparent by luminance ERG.

Further work will be needed to determine the extent of deficit at this level of the visual system.

5. REFERENCES

1. Moshos M. ERG and VER findings after laser photocoagulation of the retina. Metab Pediatr Ophthalmol 6:101 (1982).

2. Fowler BJ. Accidental industrial laser burn of the macula. Ann Ophthalmol 15:481 (1983).

3. Boldrey EE, Litle HL, Flocks M, Vassiliadis A. Retinal injury due to industrial laser burns. Ophthalmol (Rochester) 88:101 (1981).

4. Wolfe JA. Laser retinal injury. Mil Med 150:177 (1985).

5. Stuck BE, Lund DJ, Beatrice ESW. Repetitive pulse laser data and permissible exposure limits. Presidio of San Francisco, CA: Letterman Army Institute of Research. Institute Report No. 59 (1978).

6. Gibbons WD, Allen RG. Retinal damage from suprathreshold Q-switch laser exposure. Health Phy 35:461 (1978).

7. Allen RG, Thomas SJ, Harrison RF, Zuglich JA, Blankenstein MF. Ocular effects of pulsed Nd laser radiation: variation of threshold with pulsewidth. Health Phy 49:685 (1985).

8. Merigan WH, Pasternak T, Zehl D. Spatial and temporal vision in macaques after central retinal lesions. Invest Ophthalmol Vis Sci 21:17 (1981).

9. Callin GD, Devine JV, Garcia P. Visual compensatory tracking performance after exposure to flashblinding pulses: I, II, III. USAF School of Aerospace Medicine, Brooks Air Force Base, TX: Reports SAM-TR-81-3, -7, -8 (1981).

10. Randolph DI, Schmeisser ET, Beatrice ES. Grating visual evoked potentials in the evaluation of laser bioeffects: twenty nanosecond foveal ruby exposures. Am J Optom Physiol Opt 61:190 (1984).

11. Schmeisser ET. Flicker electroretinograms and visual evoked potentials in the evaluation of laser flash effects. Am J Optom Physiol Opt 62:35 (1985).

12. Schmeisser ET. Laser flash effects on laser speckle shift VEP. Am J Optom Physiol Opt 62:709 (1985).

13. Schmeisser ET. Schmeisser ET. Laser induced chromatic adaptation. Am J Optom Physiol Opt, 65: 644-652 (1988).

14. Previc FH, Blankenstein MF, Garcia PV, Allen RG. Visual evoked potential correlates of laser flashblindness in rhesus monkeys. I. Argon laser flashes. Am J Optom Physiol Opt 62:309 (1985).

15. Previc FH, Allen RG, Blankenstein MF. Visual evoked potential correlates of laser flashblindness in rhesus monkeys. II. Doubled neodymium laser flashes. Am J Optom Physiol Opt 62:626 (1985).

16. Glickman RD, Previc FH, Cartledge RM, Schmeisser ET, Zuglich JA. Assessment of visual function following laser lesions. USAFSAM Protocol # 7757-02-82 (Contract F33615-84-C-0600) (1986).

17. Schmeisser ET. Acute laser lesion effects on acuity sweep VEPs. Invest Ophthalmol Vis Sci, 1992; 33:3546-3554.

18. Westheimer G. Visual acuity and hyperacuity: resolution, localization, form. Am J Optom Physiol Opt 64:567-574 (1987).

19. Enoch JM, Williams RA. Development of clinical tests of vision: Initial data on two hyperacuity paradigms. Percept Psychophys 33:314-322 (1983).

20. Enoch JM, Essock EA, Williams RA. Relating vernier acuity and Snellen acuity in specific clinical populations. Doc Ophthalmol 58:71-77 (1984).

21. Levi DM, Manny RE, Klein SA, Steinman SB. Electrophysiological correlates of hyperacuity in the human visual cortex. Nature 306:468-470 (1983).

22. Steinman SB, Levi DM, Klein SA, Manny RE. Selectivity of the evoked potential for vernier offset. Vis Res 25:951-961 (1985).

23. Srebro R, Osetinsky MV. The localization of cortical activity evoked by vernier offset. Vis Res 27:1387-1390 (1987).

24. Enoch JM, Williams RA, Essock EA, Barricks M. Hyperacuity perimetry. Assessment of macular function through ocular opacities. Arch Ophthalmol 102:1164-1168 (1984).

25. Sutter EE, Tran D. The field topography of ERG components in man - I. The photopic luminance response. Vis Res 32:433 (1992).

26. Bearse MA, Suter EE. Imaging localized retinal dysfunction with the multifocal electroretinogram. J Opt Soc Amer A 13:634 (1996).

27. Schmeisser ET. Evaluation of retinal laser lesion healing by perimetric electroretinography. SPIE Proceedings, 2674: 108 (1996).

28. Shapley R, Victor J. Hyperacuity in cat retinal ganglion cells. Science 231: 999-1002, (1986).

29. Ringach DL, Shapley R. Spatial and temporal properties of illusory contours and amodal boundary completion. Vis Res 36: 3037-3050, (1996).

Appendix A: Fundus Photographs and Flourescein Angiogram late phases

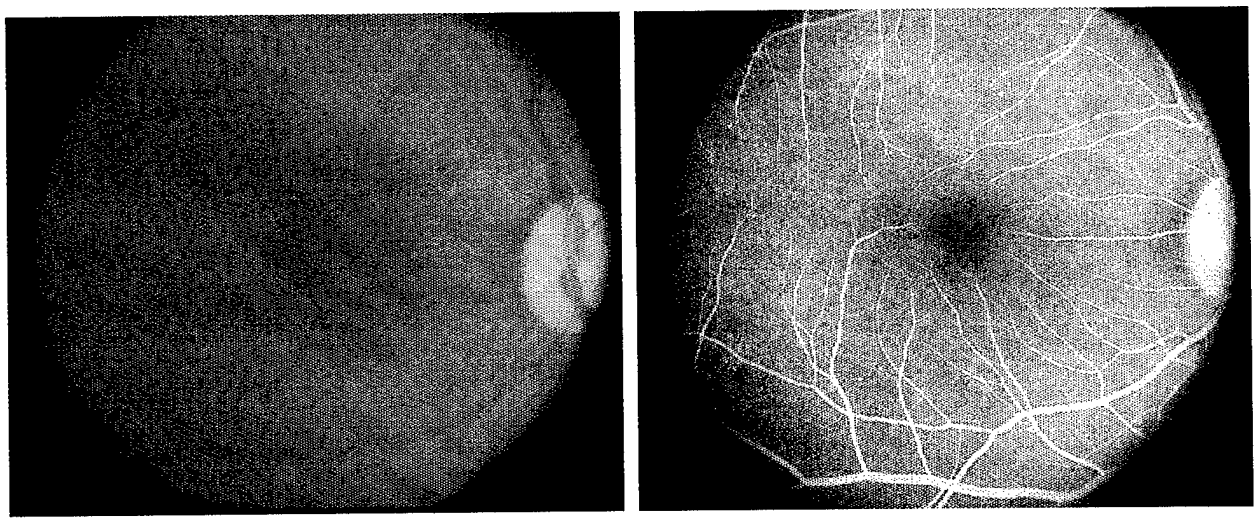

Fig . A1 & A2: CY 1141 OD (animal #1) . At the time of exposure, no lesions were noted at any of the 4 sites, even though the superior site was targeted to receive a red-dot lesion, the temporal site a white-dot and the inferior and foveal sites an MVL . The superior and temporal sites have a minor irregularities in the FA image.

Exposure parameters: temporal 01/23/91 (1B) 778 uJ; superior 02/11/91 (3A) 1772 uJ; inferior 01/09/91 (1A) 214 uJ; fovea 02/20/91 (1B) 211 uJ.

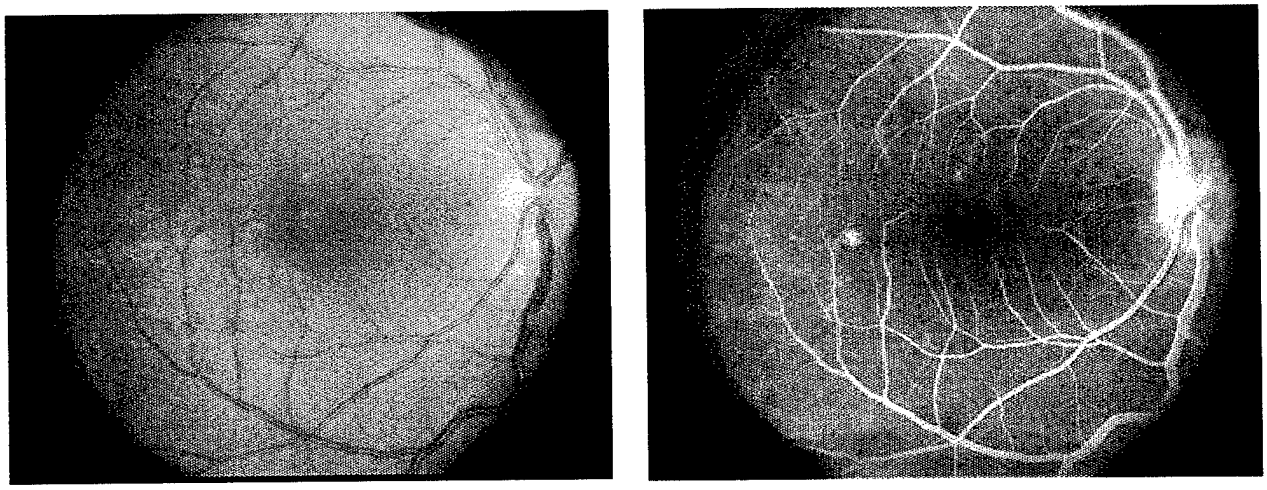

Fig . A3 & A4: CY 1136 OD (animal #2) . At the time of exposure, white-dot lesions were noted both at the temporal and the superior sites . The fovea was targeted to receive a MVL, and shows some pigmentary blanching . The superior site appears at about 4 degrees, but the temporal site appears approximately 10 degrees from the fovea . All 3 sites have FA changes as well.
Exposure parameters: temporal 01/28/91 (3A) 2181 uJ; superior 02/13/91 (1A) 224 uJ; nferior 1/14/91 (2A) 835 uJ; fovea 02/25/91 (1B) 174 uJ.

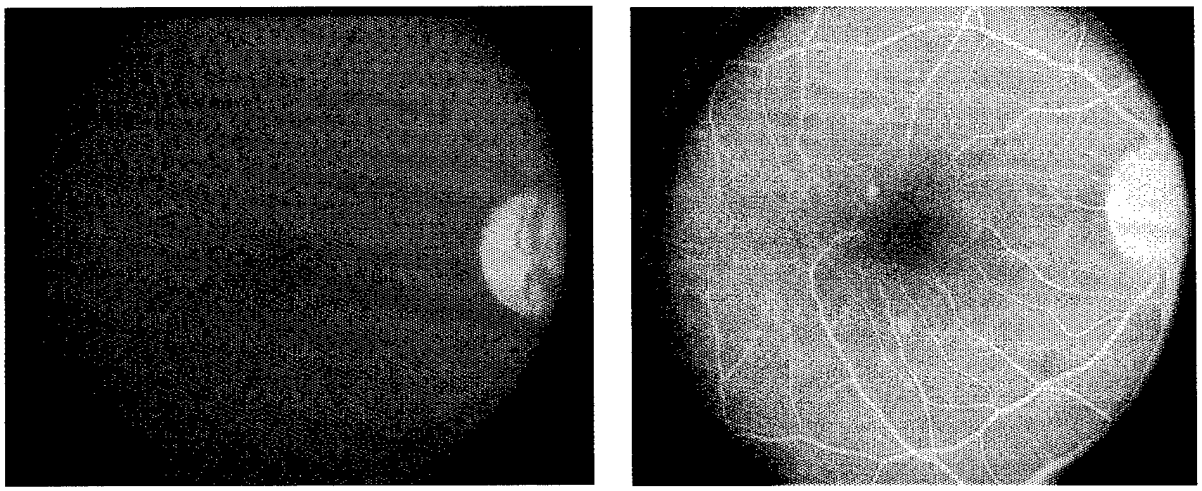

Fig . A5 & A6: CY 1507 (animal #3) . This animal shows white dot lesions about 8 degrees inferior and superior-temporally at about 5 degrees . The temporal site is clear, and the foveal site may have an MVL.

Exposure parameters: temporal 01/30/91 (1A) 202 uJ; superior 02/18/91 (2A) 751 uJ; inferior 01/16/91 (3A) 2162 uJ; fovea 02/27/91 (1B) 126 uJ.

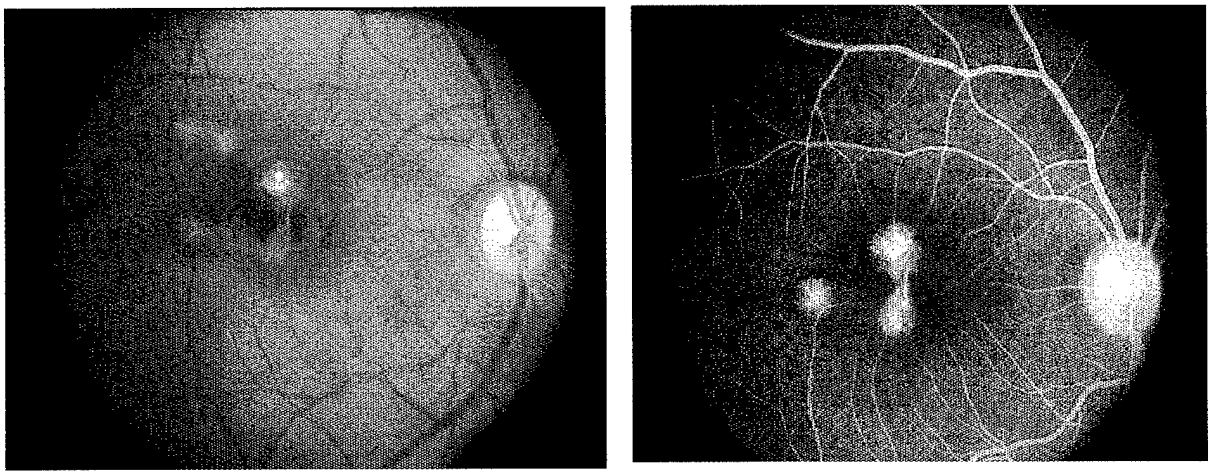

Fig . A7 & A8: CY 1159 OD (animal #4) This animal shows a bridging scar between the superior and the foveal sites (a red dot and a white dot lesion, respectively) . The temporal site also shows a white dot lesion, while the inferior site is clear. The 2 light dots in the superior temporal regions are artefacts.

Exposure parameters: temporal 03/18/91 (2A) 1051 uJ; superior 04/15/91 (3A) 3101 uJ; inferior 03/06/91 (1A) 267 uJ; fovea 03/05/91 (2B) 477 uJ.

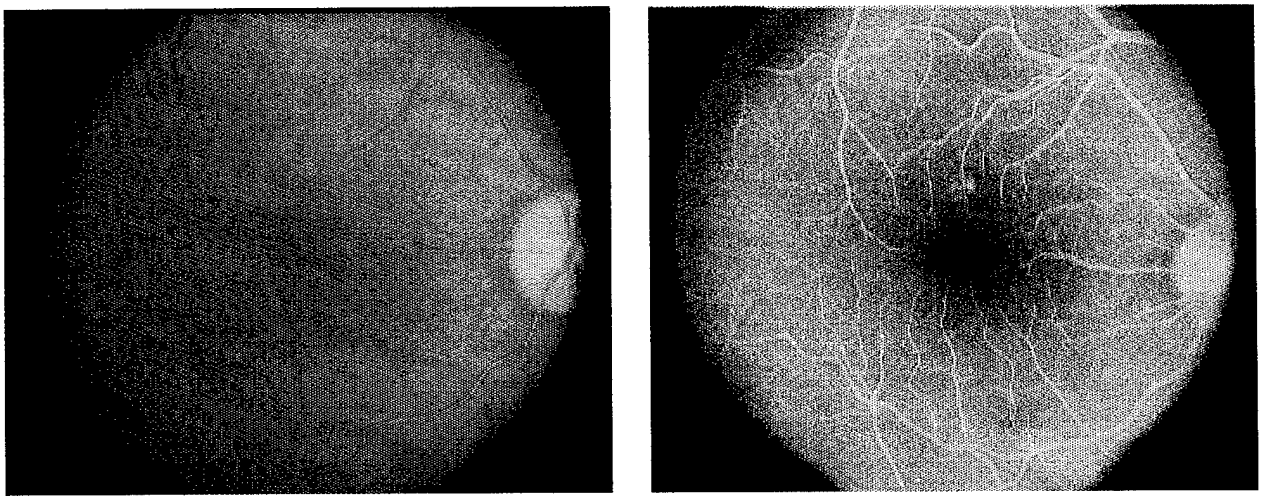

Fig . A9 & A10: CY 1209 OD (animal #7) . This animal has a circumscribed lesion (white dot) superior to the fovea . The fovea has a lesser lesion in the fundus photograph, that is not reflected in the FA, even though it was classified as a red dot lesion at the time of exposure . The temporal site is clear.

Exposure parameters: temporal 06/27/91 (2A) 1222 uJ; superior 07/11/91 (3A) 3003 uJ; inferior 06/10/91 (1A) 251 uJ; fovea 08/01/91 (3B) 1908 uJ.

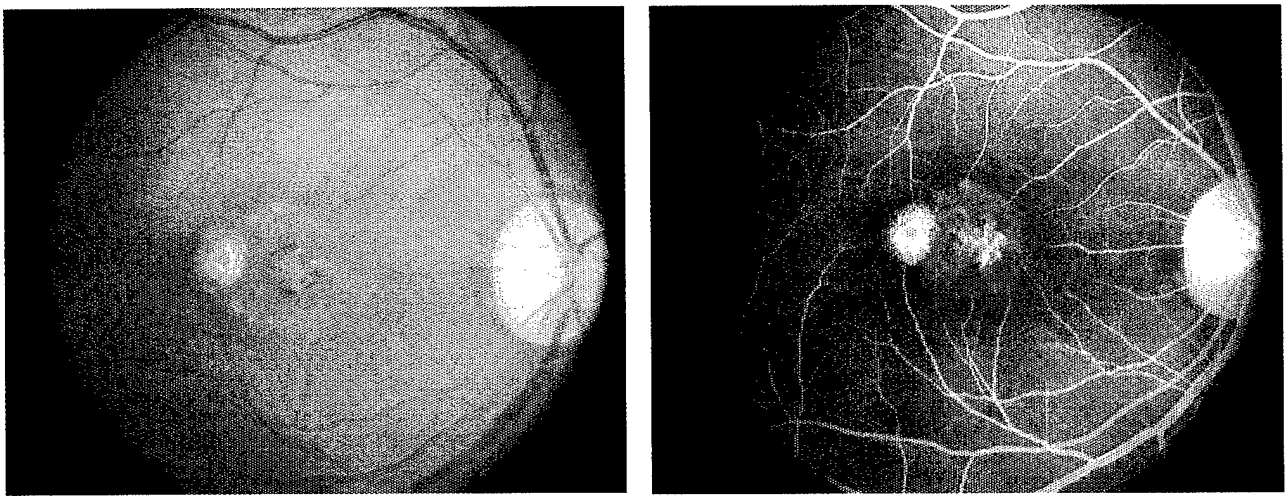

Fig . A11 & A12: CY 12029 OD (animal #8) . This animal has a red dot lesion in the fovea, and was noted at the time of exposure to have a white dot lesion temporally . Both lesions are large and a secondary ring of exudate surrounds the fovea, includes the temporal site and apparently obscures changes at the inferior and superior sites.

Exposure parameters: temporal 07/01/91 (3A) 2726 uJ; superior 07/15/91 (1A) 402 uJ; inferior 06/13/91 (2A) 1082 uJ; fovea 07/25/91 (3B) 2631 uJ.

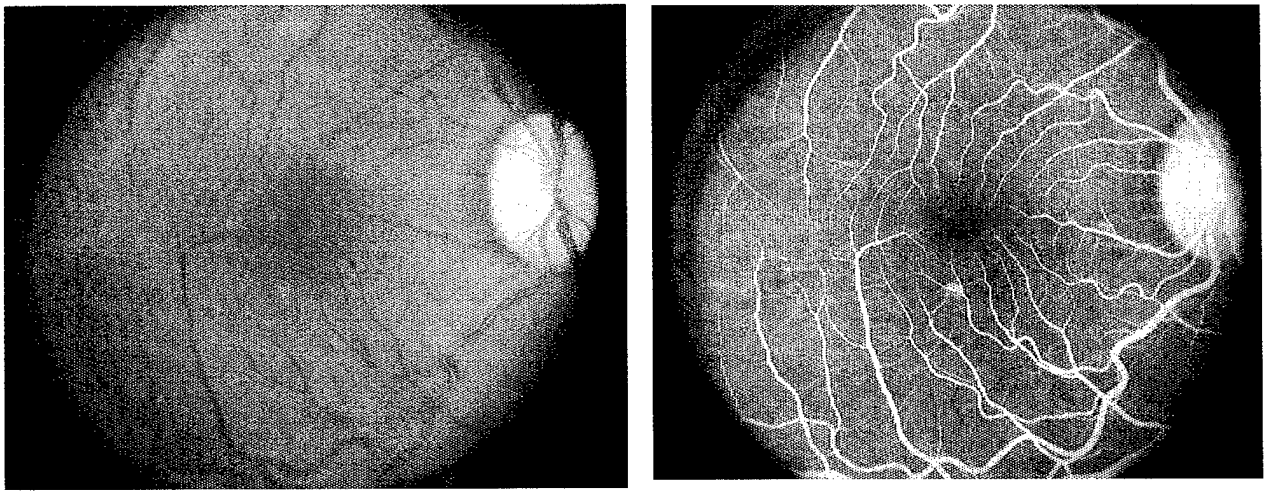

Fig . A13 & A14: CY 12043 OD (animal #9) . This animal has a foveal red dot lesion, and was noted to have an inferior white dot lesion . Both lesions remain visible, however the FA of the inferior lesion shows more severe changes . The superior site was scheduled for a white dot lesion; however no obvious changes can be noted at the site.

Exposure parameters: temporal 07/08/91 (1A) 343 uJ; superior 07/18/91 (2A) 1242 uJ; inferior 06/24/91 (3A) 2783 uJ; fovea 07/29/91 (3B) 1611 uJ.

Appendix B: Evaluation of Vernier Acuity near Healed Retinal Laser Lesions. SPIE Proceedings Series 2974: 105 - 116, 1997.

Evaluation of Vernier Acuity near Healed Retinal Laser Lesions

Elmar T. Schmeisser, Ph.D.

Dept. of Ophthalmology
E-318 Kentucky Clinic
University of Kentucky
Lexington, KY 40536-0284

ABSTRACT

Seven Cynomolgus fasciculata who had graded laser lesions placed in one eye 6 years previously were evaluated for their vernier acuity by electrophysiologic recording techniques. In these experiments, 95% contrast vernier acuity targets were presented at high luminance levels to anesthetized primates. Visual evoked potentials were recorded by conventional means from scalp electrodes through hospital grade amplifiers. All animal testing was performed under IACUC approved protocols. The single q-switched pulses from a neodymium-YAG laser had produced lesions of 4 types: no visible change, minimal visible lesions, "white dot" lesions (localized circumscribed retinal blanching) and "red dot" lesions (contained retinal hemorrhage) in the eye at the time of placement. Single exposures had been made in four locations: 5 degrees superior, inferior and temporal to the fovea, and one foveally. Vernier recording proved somewhat successful in smaller animals with less than contained retinal hemorrhage lesions in the fovea. Initial analyses demonstrated a significant decrease of the pattern response signal/noise in the experimental eye overall, and an apparent relative loss of vernier signal in some lesioned eyes. Animals with the more severe lesions have somewhat degraded small pattern responses and no recordable vernier response. Apparent lesser losses produced less effect.

Keywords: laser, retina, lesion, vernier, VEP, monkey

1. INTRODUCTION

Vision, and visual compromise due to retinal burns caused by laser exposure, has been evaluated and measured in many different ways. Visual field effects, changes in grating acuity, gray scale contrast sensitivity and chromatic sensitivity have all been measured in the attempt to quantitate a very complex sense system. In some cases, the interest was in very acute changes, while in many others, only longer term studies were possible.[1-17]

This experiment specifically investigates the ability of the visual system to make localization judgments, i.e. vernier or hyperacuity, as opposed to pattern resolution judgments, e.g. grating or letter acuities.[18] The ability of an observer to correctly judge the offset of 2 dots or line elements is quite resistant to optical degradation and is significantly different in its response to pathology.[19-20] Additionally, this ability is critical to aiming and tracking tasks common to many activities, including simply driving down the road between the lines and parking a vehicle. Visual evoked potential correlates of hyperacuity have been obtained in humans.[21-23] These studies show that the hyperacuity VEP in humans scales linearly with log offset and thus can permit estimation of the psychophysical hyperacuity threshold by extrapolation to signal amplitude extinction. However, vernier acuity

falls off with retinal eccentricity even faster than resolution acuity or contrast sensitivity.[24]

The animals used in this study have had graded laser lesions placed 6 years previously by the native collimated beam from a pulsed Nd-YAG laser emitting 1062 nm light without expansion or focusing by any lens system other than that of the eye itself. Placement and severity of these lesions was governed by attempts to produce "Wolfe grade" equivalent effects[4] with single Q-switched exposures. Four lesions had been placed in the right eye of each animal, the left eye serving as a normalizing control with no laser exposures. The exposure energy (and thus lesion type) was counterbalanced across both locations and animals for severity and only four exposures were made in the right eye of each animal. The acute effects of these lesions on acuity as measured by the sweep VEP technique have been previously reported.[17]

Summarizing the 7 animals in this experiment, at the foveal site there are 2 animals which were labeled with no visible change at the time of exposure, 2 with a "minimal visible lesion" (MVL, or Wolfe Grade 1B[4]), 2 with "white dot" lesions (retinal blanching, grade IIB) and 3 with "red dot" lesions (contained retinal hemorrhage, grade IIIB). At the parafoveal locations, there are 11 sites with no visible change at the time of exposure, 4 sites with MVL (IA), 6 sites with a white dot lesion (IIA), and 4 sites with a red dot lesion (IIIA).

Since the VEP falls off with eccentricity due to both cortical magnification and to the topographic mapping of the visual field on the cortex, the signal to noise ratio of the VEP will fall off drastically in any attempt to record a response from the periphery with noninvasive methods.[23] Accordingly, this report is limited to the examination of the vernier VEP responses when the stimulus is placed on the foveal area itself. The consideration whether isolated peripheral lesions have any additional effect to that of the foveal exposure must await a further study with different animals, although some indications are presented here.

2. METHODS

2.1 Subjects: The decision of a suitable species was driven by 3 considerations: the animal must be a primate, it must have high luminance, high acuity color vision, and its retina must have a fovea. These requirements arise from the need to model the human visual system organization (anatomy and function) both retinally and cortically in order to generalize the results of this study to human visual performance. The lowest species that would therefore be used was the cynomolgus monkey (Macaca fascicularis). Further, the recording methods are noninvasive and routinely used with human patients. All procedures were pre-approved by the university IACUC and followed the guidelines of both ARVO and the NIH.

2.2 Procedure: The animal was sedated with ketamine (10 mg/kg) supplemented with ace-promazine (1 mg/kg) IM, and then brought to the laboratory. The animal was anesthetized with pentobarbital IV (10 mg/kg) and muscularly relaxed with pancuronium bromide IV (0.025 mg/kg) as bolus doses. The pupils were dilated with 1% tropicamide and 1% neosynephrin drops. The animal then was intubated and wrapped in a warming blanket on a padded rotating stage. Temperature, ECG and pCO2 were monitored, and ventilation and blanket temperature were adjusted to maintain stable physiologic values. EEG and ECG were monitored for signs of discomfort and the anesthetic level adjusted with backup doses as needed. The fovea of one eye was

aligned in front of the fundus camera and the other eye patched closed. Each animal had been individually refracted for the stimulus distance previously and had keratometry performed to specify the appropriate contact lens parameters. This individually fitted corrective contact lens was placed on the cornea over artificial tears and the retina visualized through it. Figure 1 shows the optical layout and alignment system.[25]

After an experimental session, the animal was allowed to recover from the muscular immobilizing agent. When it could breathe unassisted, it was extubated, removed to the transfer cage and then returned to the colony under the supervision of the veterinary staff.

2.3 Stimuli, Recording and Data Processing: The hyperacuity (vernier) stimuli were produced on a square high resolution (1024 pixels squared) monochrome monitor (VisionProbe (tm)) measuring 8.35 degrees of visual angle at the eye. The stimulus was constructed of five black vertical bars 2.63 degrees tall on a white background (78 Foot-Lamberts) whose center third was horizontally offset and subsequently realigned 694 msec later (0.72 Hz), following the method of Levi *et al.*[21] A gap of 2 pixels (0.97 arcmin) was placed between each third. Each bar measured 9 pixels (4.4 arcmin) in width and was separated from its neighbors by a further 9 pixels producing an overall pattern width of 81 pixels (0.66 deg). Contrast was measured at 99.6%. The offset was counterphased between 0 and (in turn) 27, 18, 9, 4, and 2 pixels to evoke the VEP, thus covering a range from a maximum of 13.2 arcmin (approx 0.24 degrees) down to 0.98 arcmin. The VEP was recorded from bilateral occipital scalp electrodes over the foveal visual cortex individually referenced to the eyebrows (the central scalp served as signal common) in response to the each stimulus until the step size used evoked no recognizable response (generally around the 9 pixel shift size). In order to avoid any time locked activity that might obscure the signal, a random 500 msec dither was introduced between each 1 second stimulus epoch. In most cases, at least 800 sweeps acquired over multiple runs had to be averaged together and the 2 cortical channels from each animal combined in order to get a response with sufficient signal under these anesthetic and recording conditions. In addition, a set of control recordings with 8 shift/sec counter-phasing 99.6% contrast checkerboard stimuli at 1, 3 and 10 cycles/degree filling the entire monitor were used to estimate the overall visual response from each eye.

The steady state (8 Hz) checkerboard VEPs were underwent Fourier analysis and the strength of the 8 Hz component was recorded. This power spectral density, being bounded at 0, was log transformed into a normal distribution before the analysis of variance (repeated measures ANOVA by CSS Statistica, Statsoft Inc., Tulsa, OK). Signal to noise ratios (s/n) were constructed from the power of the peak pattern response divided by the average power in the 2 neighboring frequency bins. Since these ratios are bounded at 0, they were log transformed before analysis. Next, in order to create a standard comparison template, all vernier evoked potentials were normalized to the individual animal's control eye base recording (the 27 pixel shift). The averaged normalized vernier VEPs were evaluated by cross correlation limited to the time region in which the vernier component occurred (between 186 ms to 250 ms, containing the nominal P200-N220 response) both to this average template, and also between each eye for each animal. The strongest positive correlation coefficient (a Pearson's r) at the closest offset (tau) to the template response was chosen to characterize the response, i.e the closest local maximum r to tau=0. Additionally, the correlation coefficient at tau=0 was also noted. Since

correlation coefficients are not normally distributed, they also had to be transformed via the equation (known as a Fischer's transformation[26]):

$$x(r)=0.5 \ln ((1+r)/(1-r)). \quad (1)$$

From this, means and standard deviations based on the variable x can be determined, since x is approximately normally distributed. These transformed values were then compared by repeated measures ANOVA and the effects of the lesions extracted. For graphical purposes, normal ranges can be obtained with these values (e.g. +/- 2 S.D.), and then back transformed to provide normal boundaries on a graph of r vs tau (the lead/lag amount) via the inverse of equation 1 as follows:

$$r=1-2/(\exp(2x)+1). \quad (2)$$

These equations coupled with the cross correlation analysis provides an relatively objective method of statistically determining the presence of any reliable response (i.e. the VEP), rather than having to judge which "squiggle" is the actual response component.

3. RESULTS

One of the animals (12043, a large male) had pattern VEPs in the control eye which at the base stimulus (1 c/d checkerboard) were too small to be useful; this animal's data was eliminated. Further, two other animals (1209 and 12029) had no reliable vernier VEPs even to the largest offset in the control eye (correlation coefficients with the template were consistently negative), and so were dropped from the vernier analyses. In order to attempt a statistical analysis with the remaining few animals, the experimental eyes were grouped roughly as those with no lesions to minimally visible foveal lesions (2 animals), and those with severe or scarring foveal lesions (2 animals). All comparisons were made against their paired control eye (repeated measures ANOVA). Both the x(r) at tau=0 and the x(r)max with the coupled tau at x(r)max as a covariate were analyzed as a function of lesion class (minimal vs white or red dot) with both eye and offset as the repeated measures. More quantitative characterization of the lesions will have to await fluorescein angiography, topographic retinal response mapping by ERG, detailed scanning laser ophthalmoscopy and postmortem histology.

Fig. 2 shows the normalized summed averages series of VEP responses from the normal control eyes (OS) and from all the fellow laser exposed eyes (OD) elicited by 3 checkerboard stimuli of differing check sizes. As can be seen, the lesioned side has pattern VEP responses down to 10 cycles per degree that appear similar to the control eye. Despite the small number of animals, statistical analysis of the signal to noise ratios derived from the power spectral densities of the steady state pattern VEPs showed that as a class, the more severely exposed eyes have lower log(s/n) than the normal eyes (P=0.036); however overall response power itself was not significantly different as a function of either eye, or exposure class (see fig. 4). There was a tendency towards more severe effects with more severe lesions, but this did not attain significance (p=0.27). Spatial frequency was as expected a significant factor (P=0.005) with the lowest spatial frequency demonstrating a stronger response than the smaller patterns.

Fig. 4 shows foveal vernier VEP responses from one animal, demonstrating that even with large offsets, the response decreases in the lesioned eye while remaining recordable from the control eye. Analysis of the maximum crosscorrelation results (with the corresponding tau set as a covariate) demonstrated no significant effects due to eye, class or vernier offset, even though the trends were as expected (lower correlation with smaller offsets, in the lesioned eye and with more severe lesions). For example, comparison of the data between exposure classes (minimal vs white or red lesions) in the experimental eye demonstrated a tendency towards more severe losses of correlation with the more severe lesion, but the effect did not attain significance ($p=0.152$). In contrast, examination of the correlation results with no offset in time (fig. 5) showed an interaction effect between lesion class and eye ($p=0.041$). Looking at only the exposed eye and analyzing for the effect of lesion class across all vernier offsets, the more severe lesion was significantly more effective in dropping the response ($p=0.033$). Finally, there is a tendency for the interocular correlation to drop with the more severe lesions, but this did not attain significance in this small sample ($p=0.13$).

Off-axis burns (5 degree) did not seem to affect vernier acuity in these particular long term animals, e.g. one animal with an apparent MVL in the fovea but with white and red dot lesions in periphery has vernier VEP responses that are equivalent between the 2 eyes.

4. DISCUSSION

The decrease in signal to noise ratio in the relatively large field pattern VEPs without a concomitant loss of absolute response power in intriguing. Does an abnormal fovea actually increase the visual system's noise as opposed to simply removing its contribution to the response? This type of masking or interference may have functional consequences that extends beyond the apparent lesion diameter, and would need to be separately considered. On the other hand, the data presented here does not support the inverse idea, viz. that damaged peripheral retina has a significant ability to affect foveal function as measured by pattern VEP.

The comparison between the responses to checkerboard stimuli and vernier stimuli of a comparable size indicates that the vernier response is probably even more sensitive to retinal disruption, a finding in opposition to that noted with optical compromise. This might be expected, since the pattern VEP responses were obtained with stimuli that covered normal as well as abnormal retina, but the localized vernier stimuli may not have impinged on unexposed retina, and in the case of the most severe lesions, may not extend outside a presumed local scotoma. Topographic mapping studies using electroretinography[27] are in progress and should clarify the extent of these effects. Other data exists that implicates retinal ganglion cells as being the limiting factor in vernier resolution.[28] While this data was obtained in cats rather than primates, if the physiological mechanism holds across species, the apparent damage to vernier acuity with the current laser lesions implies that the cortex may not be able to compensate for these retinal signal losses, unlike the image filling in or illusory border completion that can occur with more extended patterns.[29] In summary, the vernier VEP analyses imply that for any offset size, including those well above normal vernier threshold, 1) there tends to be a drop due to any foveal exposure, and 2) this drop appears to be more severe with greater lesions.

It should be reiterated that not all animals produced recordable vernier VEPs with this protocol, even from their normal eyes. This tended especially to be the case for the larger (male) animals and may be an artefact of their greater skull thickness and head musculature combined with the small size of the signal when recorded by surface (either subcutaneous needle or scalp cup) EEG electrodes. In order to improve this situation, implantation of chronic electrodes to record from at least the dural surface probably would be required.[30] Finally, an exhaustive perilesional mapping protocol in order to maximize any vernier signal by placing it just outside of a (presumed) lesion scotoma was not undertaken. Behavioral studies which would allow the animal to adopt individual compensatory strategies (such as off axis viewing with alternate preferred retinal loci) might be more appropriate to determine the final functional consequences of discrete retinal lesions such as those in this study.

5. ACKNOWLEDGMENTS

This work was supported in part by funds under USAMRMC Contract No. DAMD17-95-C-5038, Ft. Detrick, MD, by funds from The Analytic Sciences Corporation, Reading, MA, equipment from the Armstrong Laboratories and from the US Army Medical Research Detachment (WRAIR), both of Brooks AFB, TX, and by an unrestricted departmental grant from Research to Prevent Blindness, Inc.

6. REFERENCES

1. Moshos M. ERG and VER findings after laser photocoagulation of the retina. Metab Pediatr Ophthalmol 6:101 (1982).

2. Fowler BJ. Accidental industrial laser burn of the macula. Ann Ophthalmol 15:481 (1983).

3. Boldrey EE, Litle HL, Flocks M, Vassiliadis A. Retinal injury due to industrial laser burns. Ophthalmol (Rochester) 88:101 (1981).

4. Wolfe JA. Laser retinal injury. Mil Med 150:177 (1985).

5. Stuck BE, Lund DJ, Beatrice ESW. Repetitive pulse laser data and permissible exposure limits. Presidio of San Francisco, CA: Letterman Army Institute of Research. Institute Report No. 59 (1978).

6. Gibbons WD, Allen RG. Retinal damage from suprathreshold Q-switch laser exposure. Health Phy 35:461 (1978).

7. Allen RG, Thomas SJ, Harrison RF, Zuglich JA, Blankenstein MF. Ocular effects of pulsed Nd laser radiation: variation of threshold with pulsewidth. Health Phy 49:685 (1985).

8. Merigan WH, Pasternak T, Zehl D. Spatial and temporal vision in macaques after central retinal lesions. Invest Ophthalmol Vis Sci 21:17 (1981).

9. Callin GD, Devine JV, Garcia P. Visual compensatory tracking performance after exposure to flashblinding pulses: I, II, III. USAF School of Aerospace Medicine, Brooks Air Force Base, TX: Reports SAM-TR-81-3, -7, -8 (1981).

10. Randolph DI, Schmeisser ET, Beatrice ES. Grating visual evoked potentials in the evaluation of laser bioeffects: twenty nanosecond foveal ruby exposures. Am J Optom Physiol Opt 61:190 (1984).

11. Schmeisser ET. Flicker electroretinograms and visual evoked potentials in the evaluation of laser flash effects. Am J Optom Physiol Opt 62:35 (1985).

12. Schmeisser ET. Laser flash effects on laser speckle shift VEP. Am J Optom Physiol Opt 62:709 (1985).

13. Schmeisser ET. Laser flash effects on chromatic discrimination in monkeys. USAFSAM TR-87-17, Brooks Air Force Base, TX (1987).

14. Previc FH, Blankenstein MF, Garcia PV, Allen RG. Visual evoked potential correlates of laser flashblindness in rhesus monkeys. I. Argon laser flashes. Am J Optom Physiol Opt 62:309 (1985).

15. Previc FH, Allen RG, Blankenstein MF. Visual evoked potential correlates of laser flashblindness in rhesus monkeys. II. Doubled neodymium laser flashes. Am J Optom Physiol Opt 62:626 (1985).

16. Glickman RD, Previc FH, Cartledge RM, Schmeisser ET, Zuglich JA. Assessment of visual function following laser lesions. USAFSAM Protocol # 7757-02-82 (Contract F33615-84-C-0600) (1986).

17. Schmeisser ET. Acute laser lesion effects on acuity sweep VEPs. Invest Ophthalmol Vis Sci, 1992; 33:3546-3554.

18. Westheimer G. Visual acuity and hyperacuity: resolution, localization, form. Am J Optom Physiol Opt 64:567-574 (1987).

19. Enoch JM, Williams RA. Development of clinical tests of vision: Initial data on two hyperacuity paradigms. Percept Psychophys 33:314-322 (1983).

20. Enoch JM, Essock EA, Williams RA. Relating vernier acuity and Snellen acuity in specific clinical populations. Doc Ophthalmol 58:71-77 (1984).

21. Levi DM, Manny RE, Klein SA, Steinman SB. Electrophysiological correlates of hyperacuity in the human visual cortex. Nature 306:468-470 (1983).

22. Steinman SB, Levi DM, Klein SA, Manny RE. Selectivity of the evoked potential for vernier offset. Vis Res 25:951-961 (1985).

23. Srebro R, Osetinsky MV. The localization of cortical activity evoked by vernier offset. Vis Res 27:1387-1390 (1987).

24. Enoch JM, Williams RA, Essock EA, Barricks M. Hyperacuity perimetry. Assessment of macular function through ocular opacities. Arch Ophthalmol 102:1164-1168 (1984).

25. Blankenstein MF, Previc FH. Approximate visual axis projection for the rhesus monkey using a fundoscope and alignment laser. Vis Res 25: 301-305, (1985).

26. Kendall MG, Stuart A. The advanced theory of statistics, Vol 1. Hafner Publ Co., New York, NY, pp 390-392 (1963).

27. Bearse MA Jr, Sutter EE. Imaging localized retinal dysfunction with the multifocal electroretinogram. J Opt Soc Am A 13: 634-642, (1996).

28. Shapley R, Victor J. Hyperacuity in cat retinal ganglion cells. Science 231: 999-1002, (1986).

29. Ringach DL, Shapley R. Spatial and temporal properties of illusory contours and amodal boundary completion. Vis Res 36: 3037-3050, (1996).

30. Schmeisser ET. Laser induced chromatic adaptation. Am J Optom Physiol Opt, 65: 644-652 (1988).

7. FIGURES

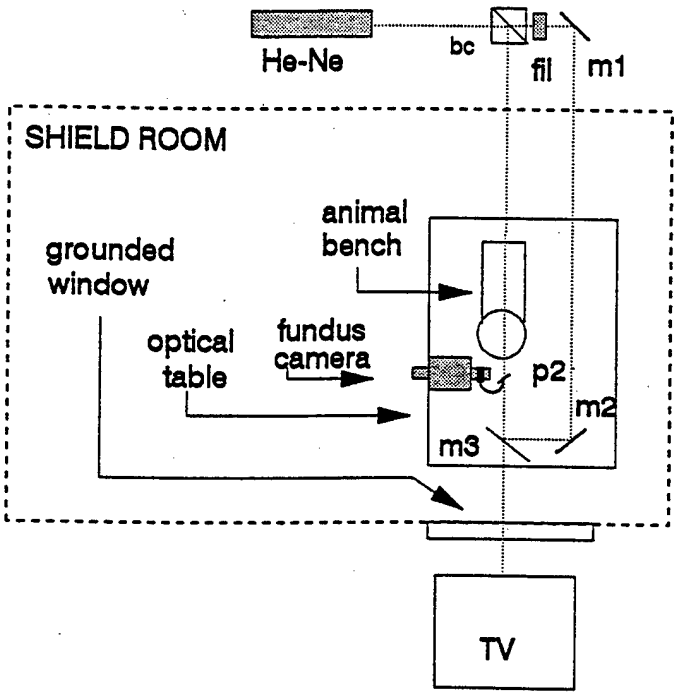

Fig. 1: Layout of the optical alignment system used in this study. He-Ne: alignment laser; bc: beam splitter cube; m1, m2 & m3: mirrors (m3 can be moved from the line of sight); p2: removable 80% reflecting pellicle.

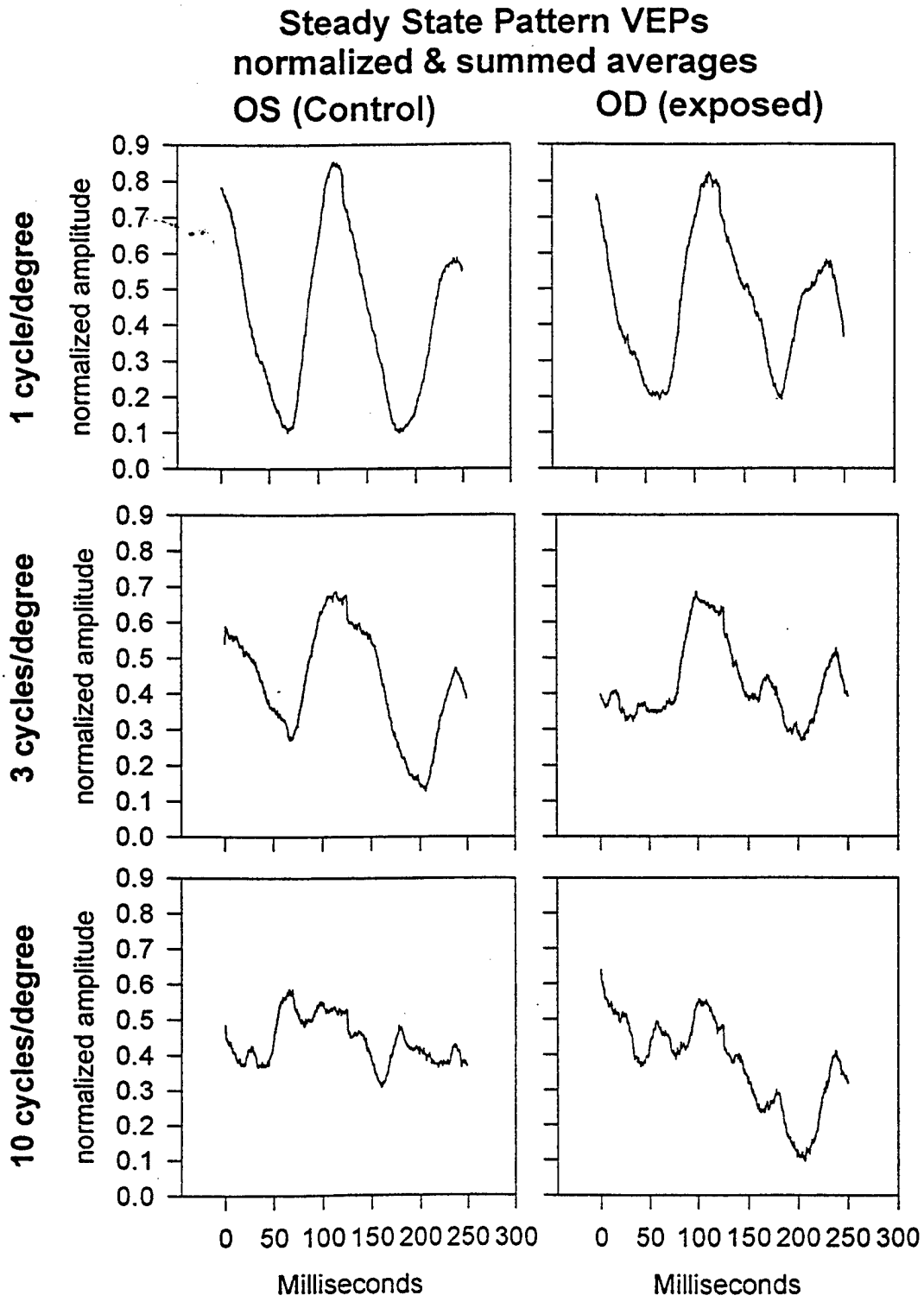

Fig. 2: Summed and averaged VEPs from checkerboard stimulation. Data combined across all animals.

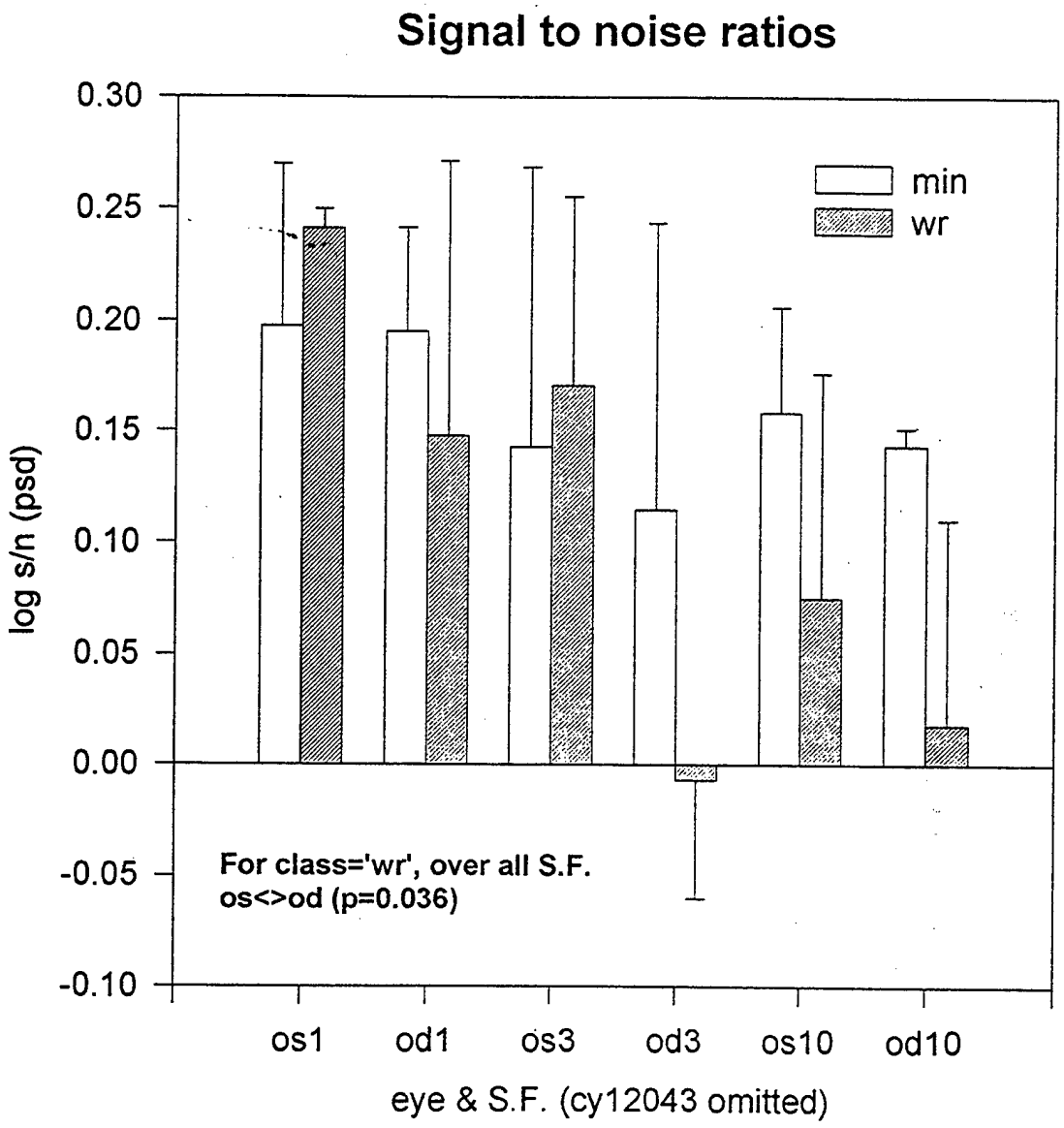

Fig. 3: Data graph of signal to noise ratios as noted in text. For those animals with white or red dot lesions, the exposed eye has a significantly worse s/n than the control eye (p=0.036).

114

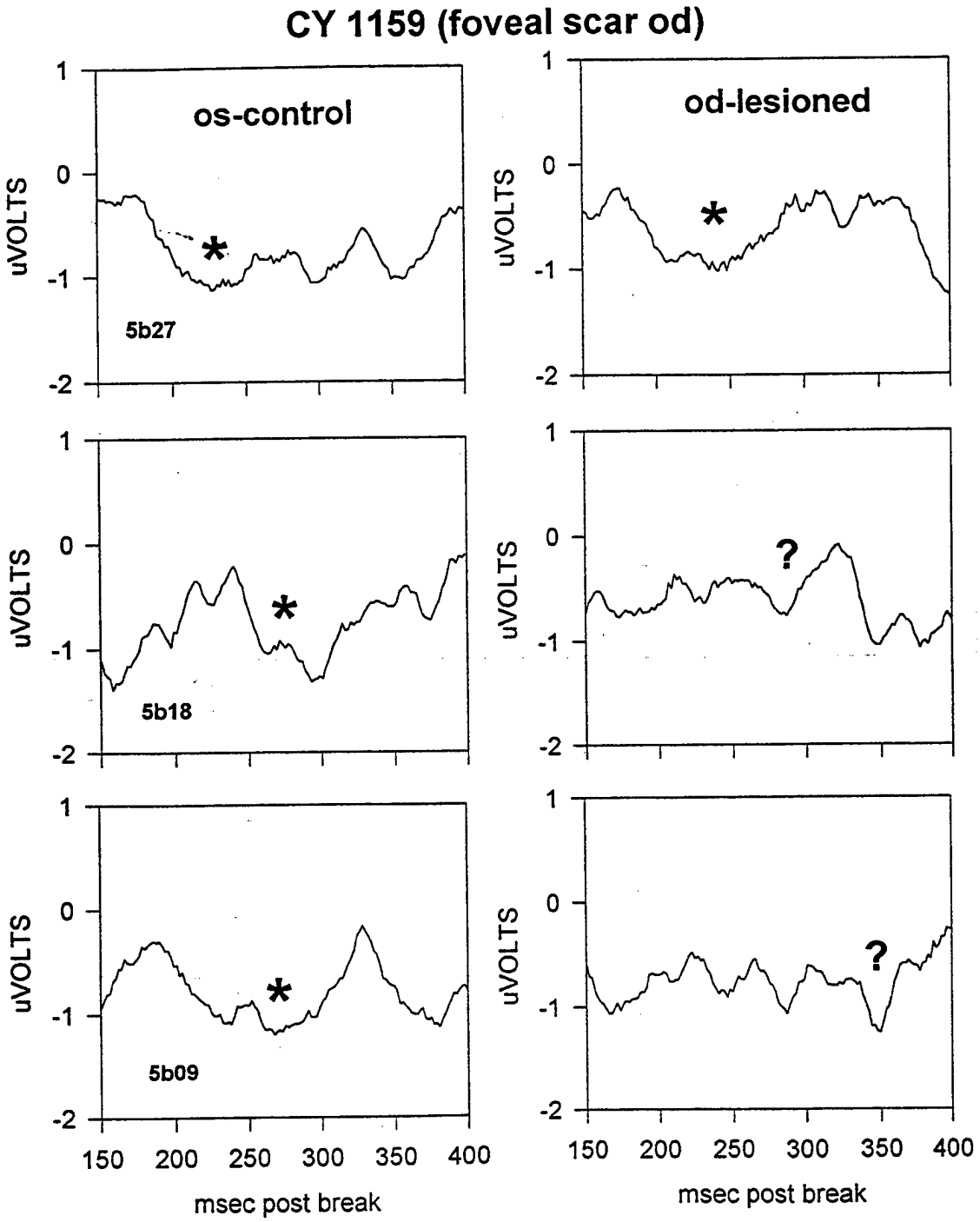

Fig. 4: VEPs from vernier stimulation for animal cy1159, which has a foveal bridging scar OD.

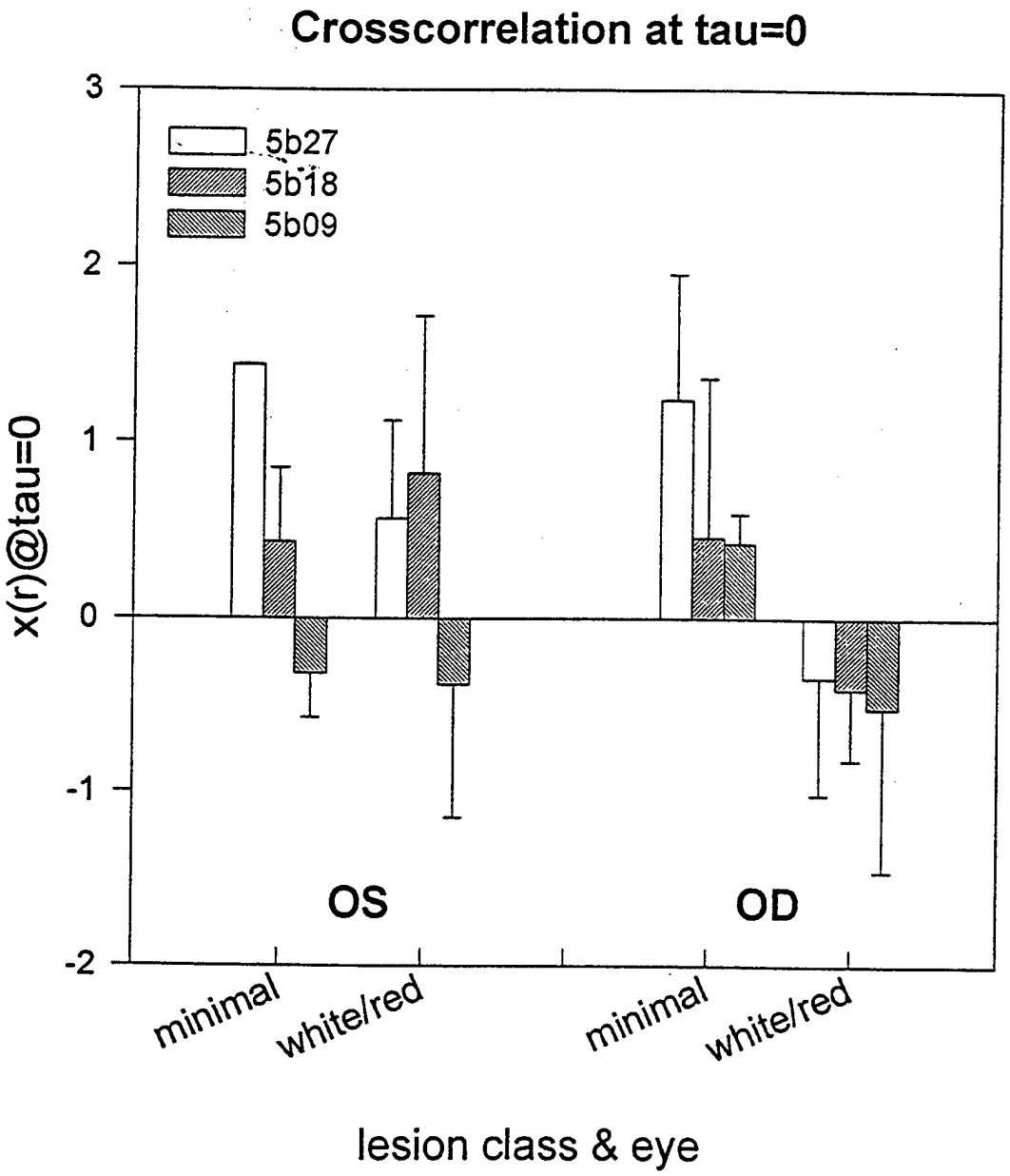

Fig. 5: Data graph of cross correlation results with no time offset against the 5b27 OS template. For those animals with white or red dot lesions, the exposed eye has a significantly lower correlations than the control eye (p=0.033).

Appendix C: Evaluation of Retinal Laser Lesion Healing by Perimetric Electroretinography: Update. Lasers in the Modern Battlefield Conference 26, 1997.

Evaluation of retinal laser lesion healing by perimetric electroretinography: update

Elmar T. Schmeisser, Ph.D.
Director, Visual Functions Clinic
Associate Professor of Ophthalmology
University of Kentucky
E-318 Kentucky Clinic
Lexington, KY 40536-0284

ABSTRACT

Seven Cynomolgus fasciculata who had graded laser lesions placed in one eye 6 years previously were evaluated by a stimulation and electrophysiologic recording technique to produce maps of retinal function. All animal testing was performed under IACUC approved protocols. The single q-switched pulses from a neodymium-YAG laser produced lesions of 4 types: no visible change, minimal visible lesions, "white dot" lesions (localized circumscribed retinal blanching) and "red dot" lesions (contained retinal hemorrhage) in the eye at the time of placement. Single exposures had been made both foveally and at 5 degrees eccentricity in the parafovea superiorly, inferiorly and temporally in one eye only. The multifocal (perimetric) electroretinogram was recorded from specialized contact lenses through hospital grade amplifiers. Optimization of recording parameters resulted in repeatable maps of the central retina. Lesions were demonstrable, especially in the foveal "red dot" cases, although the amount of signal decrement was not severe. Histological follow-up will be needed to determine if there has been receptor migration into the lesion sites during the healing process.

Keywords: electroretinogram, healing, laser, neodymium, perimetry, primate, retina, q-switch, Wolfe grade.

1. INTRODUCTION

Previous studies both by this author and many others have examined the effect of laser exposures on the electrophysiological responses of the retina.[1-9] Long term studies on the functional recovery of the retina subjected to discrete laser lesions have not been completed, nor are most techniques available suitable for noninvasive examination of small disjunct retinal areas. Over the past few years, an innovative experimental technique has been introduced that may help to address this problem: multi-input electroretinography.[10,11] This method uses a tiled stimulus display in which each hexagonal tile is flickered independently such that the overall averaged luminance change is zero and each tile has a unique temporal signature (the m-sequence technique). The ERG is recorded to this multiple stimulus from a single recording electrode and then cross-correlated to each tile's individual signature. This results in a topographic or perimetric map of the retinal response which seems to correlate with ganglion cell density across the

retina. A previous attempt by the author to use this technique was unable to produce sufficient signal/noise enhancement to provide reliable data.[12] These problems have now been solved.

2. METHODS

2.1 Subjects All procedures were pre-approved by the university IACUC and followed the guidelines of both ARVO and the NIH. The cynomolgus monkeys (Macaca fascicularis) that were used in this study have been housed in AAALAC approved facilities since their laser exposures in 1991. All recording methods were noninvasive and are routinely used with human patients.

Graded laser lesions had been placed 6 years prior to this study by the native collimated beam from a pulsed Nd-YAG laser emitting 1062 nm light without expansion or focusing by any lens system other than that of the eye itself. Placement and severity of these lesions was governed by attempts to produce "Wolfe grade" equivalent effects[13,14] with single Q-switched exposures. Summarizing the animals in this experiment, there are 2 foveal sites which were labeled with no visible change at the time of exposure, 2 with a "minimal visible lesion" (MVL, or Wolfe Grade 1B[13]), 2 with "white dot" lesions (retinal blanching, grade IIB) and 3 with "red dot" lesions (contained retinal hemorrhage, grade IIIB). At the parafoveal locations, there are 11 sites with no visible change at the time of exposure, 4 sites with MVL (IA), 6 sites with a white dot lesion (IIA), and 4 sites with a red dot lesion (IIIA). Their current appearance varies, in some cases drastically, from the grading at the time, ranging from some "red dot" lesions almost vanishing to now relatively prominent "minimally visible" lesions.

2.2 Stimulus and Recording The stimulus was produced by a specially designed Nu-Bus video board hosted in a Macintosh Quadra 650 computer. Two multi-sync monitors are attached (one 14 inch stimulus monitor and one console monitor) and data was acquired by an analog to digital converter also housed in the same computer. The raw signal was recorded from corneal contact lens electrodes and preamplified with hospital grade amplifiers before being fed to the computer. Amplifiers were set to a gain of 200,000 with a bandpass of 3 - 100 Hz. The specially written software package (VERIS^{tm}) simultaneously updates multiple areas on the stimulus monitor while synchronously acquiring the electrophysiological data and calculating the next m-sequence set. This system is available from the developer, Dr. Erich Sutter (Smith-Kettlewell Eye Research Institute, 2232 Webster St., San Francisco, CA 94115).

Each retina was mapped with a 61 element, equal area hexagonal stimulus pattern placed at 81.3 cm distance and centered on the fovea. This arrangement resulted in approximately 1.5 degree resolution in the 16 degree diameter perimetric maps. Using software interpolation, the resolution essentially can be doubled.

2.3 Procedure The animal was brought to the laboratory, sedated and premedicated with ketamine IM. The pupils were dilated with 1% epinephrine and 1% tropicamide drops. The ERG lens was test fitted to each eye, and a correcting lens was selected by streak retinoscopy to correct for the monitor to eye distance and any optical ametropia. The animal was anesthetized with Nembutal IV (10 mg/kg) and muscularly relaxed with pancuronium bromide IV (0.025 mg/kg) as bolus doses. The animal then was intubated, placed in front of the fundus camera on a padded rotating stage, and wrapped in a warming blanket. Temperature, ECG and pCO2 was monitored; ventilation and blanket temperature were adjusted to maintain physiologic values. EEG and ECG were monitored for signs of discomfort and the anesthetic level adjusted with backup doses as needed. The ERG contact lens electrode was replaced on the cornea over viscous artificial tears (Goniosol^{tm}) and the retina visualized through it. Following alignment of the fovea with the fundus camera crosshairs, the previously individually selected correcting lens was placed in front of the contact lens to bring the monitor screen into focus on the retina, using the alignment laser back reflections for centration. Figure 1 shows the optical layout and alignment system.[15] ERG maps were calculated from an 8 min long m-sequence acquisition. At least 2 and generally 4 maps were made in each eye to determine repeatability. Response data for each animal's eye was averaged over the repeated maps for final analysis.

After an experimental session, the animal was allowed to recover from the muscular immobilizing agent. When it could breathe unassisted, it was extubated, removed to the transfer cage and then returned to the colony under the supervision of the veterinary staff.

RESULTS

All ERG maps of eyes with obvious discrete lesions showed remarkably small circumscribed areas of somewhat reduced response, even in those retinas noted as having "red dot" lesions at the time of placement. Visually, the 3-dimensional maps appeared to be "volcano" shaped rather than showing a more or less smooth "hill of vision". The caldera of this volcano averaged about a 10% drop in response compared to the areas immediately adjacent. The most severe drop was of approximately 25% in one eye with a bridging scar between the foveal site and the superior site. Fig. 2 shows the fundus image of this eye, fig. 3 the trace array, and fig. 4 the coded map (gray scale in this paper). Fig. 5 shows the 3-dimensional topographic representation of the ERG responses and fig. 6 shows a profile of relative response amplitudes through the center of the response decrement, and demonstrates the above mentioned 25% drop. Most of the maps also showed some edge artefacts (loss of signal), especially in the inferior field that may have been due to partial occlusion of the upper edge of the pupil by the central recording element in the contact lens. As a result, mapping of the peripheral lesions may have to be done explicitly. Lesions of the

MVL type were not clearly apparent, nor were all the white dot type lesions.

DISCUSSION

In contrast to the previous report of results with these animals using this technique,[12] further work has shown that there are three prerequisites for successful recording: 1) good oculostasis, insured by pentobarbital and pancuronium medication, 2) a well fitted nonglaring bipolar ERG contact lens with the correct contact lens curvature as well as acceptable electrical and optical properties, and 3) refraction by streak retinoscopy over the contact lens to correct both for the stimulus distance and the animal's own refractive error, if any, as well as for the lens induced changes.

It should be noted that each map took 8 minutes to acquire, and several maps were averaged to obtain the data. Some eye drift was bound to occur since the recordings were not made under optically stabilized conditions, nor under infrared visual monitoring. As a result, the response profiles may be somewhat shallower and the actual limits of the response losses less distinct than may be in fact the case. However, this drift could only have been on the order of a few degrees since the alignment was checked before and after the series of runs, and in most cases seemed stable to visual inspection. Nevertheless, that there is as much signal as was seen in these cases implies that these focal lesions do not have a wide spread effect on the entire retina, nor that all luminance processing close by, if not at, the lesions site is destroyed. Whether this retention of signal generating ability is due to the healing process, e.g. photoreceptor migration into the lesion site, must await histological recovery of the tissue.

A final point concerns the possibility of deeper functioanl deficits when the visual system is queried with more demanding stimuli, e.g. patterns. This is best done electrophysiologically with the visual evoked potential (VEP). A few maps were obtained that seemed to indicate that the VEP can demonstrate lesions that are not apparent by luminance ERG. Further work will be needed to determine the extent of deficit at this level of the visual system.

ACKNOWLEDGMENTS

This work was supported in part by funds under USAMRMC Contract No. DAMD17-95-C-5038, Ft. Detrick, MD, by funds from The Analytic Sciences Corporation, Reading, MA, equipment from the Armstrong Laboratories and from the US Army Medical Research Detachment (WRAIR), both of Brooks AFB, TX, and by an unrestricted departmental grant from Research to Prevent Blindness, Inc. Dr. William Hare of Allergan Pharmaceuticals, Inc. (Irvine, California) is also gratefully acknowledged for his technical advice in this project.

REFERENCES

1. Moshos M. ERG and VER findings after laser photocoagulation of the retina. Metab Pediatr Ophthalmol 6:101 (1982).

2. Randolph DI, Schmeisser ET, Beatrice ES. Grating visual evoked potentials in the evaluation of laser bioeffects: twenty nanosecond foveal ruby exposures. Am J Optom Physiol Opt 61:190 (1984).

3. Schmeisser ET. Flicker electroretinograms and visual evoked potentials in the evaluation of laser flash effects. Am J Optom Physiol Opt 62:35 (1985).

4. Schmeisser ET. Laser flash effects on laser speckle shift VEP. Am J Optom Physiol Opt 62:709 (1985).

5. Schmeisser ET. Laser flash effects on chromatic discrimination in monkeys. USAFSAM TR-87-17, Brooks Air Force Base, TX (1987).

6. Previc FH, Blankenstein MF, Garcia PV, Allen RG. Visual evoked potential correlates of laser flashblindness in rhesus monkeys. I. Argon laser flashes. Am J Optom Physiol Opt 62:309 (1985).

7. Previc FH, Allen RG, Blankenstein MF. Visual evoked potential correlates of laser flashblindness in rhesus monkeys. II. Doubled neodymium laser flashes. Am J Optom Physiol Opt 62:626 (1985).

8. Glickman RD, Previc FH, Cartledge RM, Schmeisser ET, Zuglich JA. Assessment of visual function following laser lesions. USAFSAM Protocol # 7757-02-82 (Contract F33615-84-C-0600) (1986).

9. Schmeisser ET. Acute laser lesion effects on acuity sweep VEPs. Invest Ophthalmol Vis Sci 33:3546-3554 (1992).

10. Sutter EE, Tran D. The field topography of ERG components in man - I. The photopic luminance response. Vis Res 32:433 (1992).

11. Bearse MA, Suter EE. Imaging localized retinal dysfunction with the multifocal electroretinogram. J Opt Soc Amer A 13:634 (1996).

12. Schmeisser ET. Evaluation of retinal laser lesion healing by perimetric electroretinography. SPIE Proceedings, 2674: 108 (1996).

13. Wolfe JA. Laser retinal injury. Mil Med 150:177 (1985).

14. American National Standards Institute. Safe use of lasers, ANSI Z - 136.1 - 1980. New York: American National Standards Institute (1980).

15. Blankenstein MF, Previc FH. Approximate visual axis projection for the rhesus monkey using a fundoscope and alignment laser. Vis Res 25: 301 (1985).

FIGURES

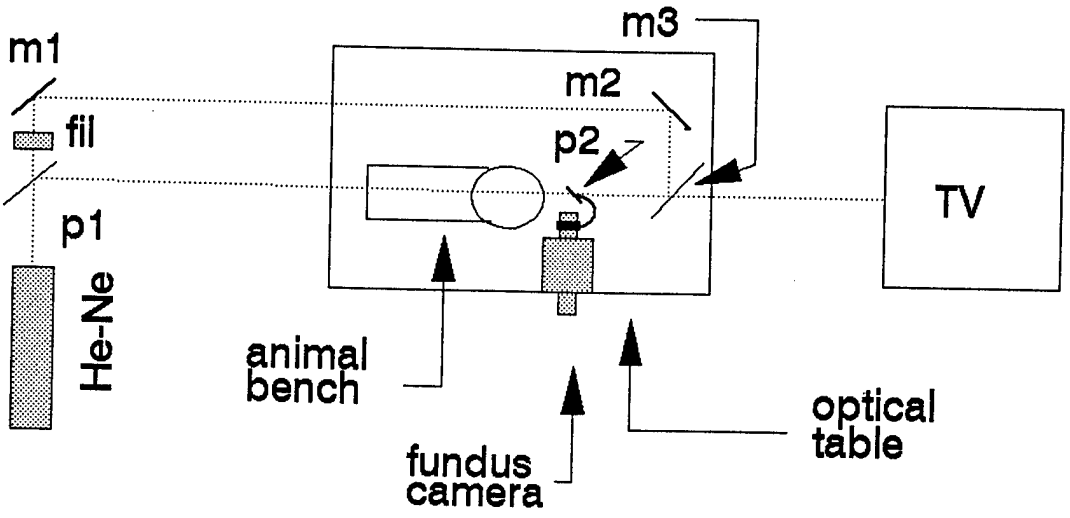

Fig.1: Layout of the optical alignment system used in this study. He-Ne: alignment laser; bc: beam splitter cube; m1, m2 & m3: mirrors (m3 can be moved from the line of sight); p2: removable 80% reflecting pellicle.

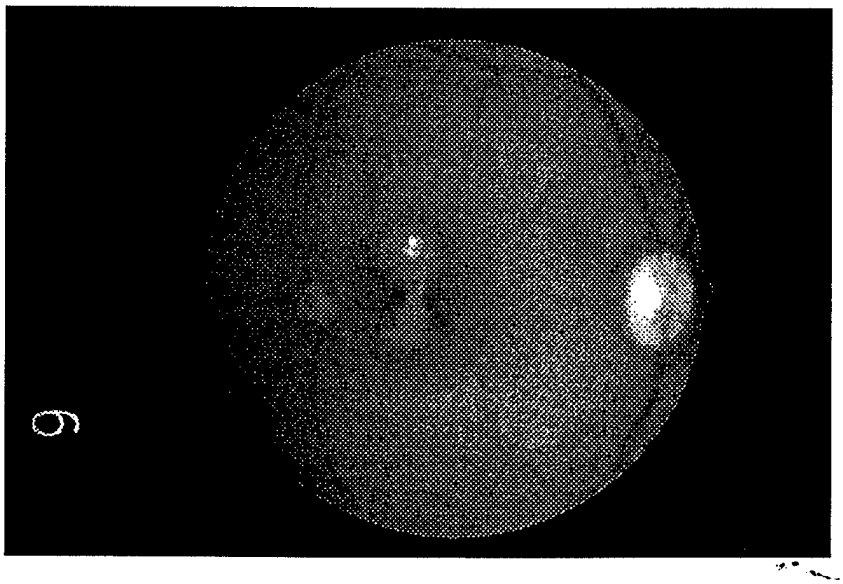

Fig. 2. Fundus picture of CY 1159 showing the bridging scar between lesions in the fovea and 5 degrees superior. A lesion is also visible in the near temporal retina; the inferior site seems clear.

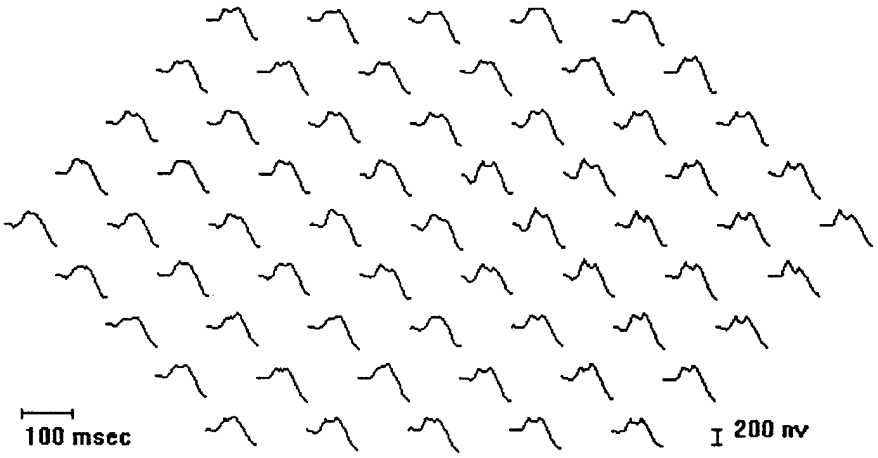

Fig. 3. Average trace array from the eye in fig. 2.

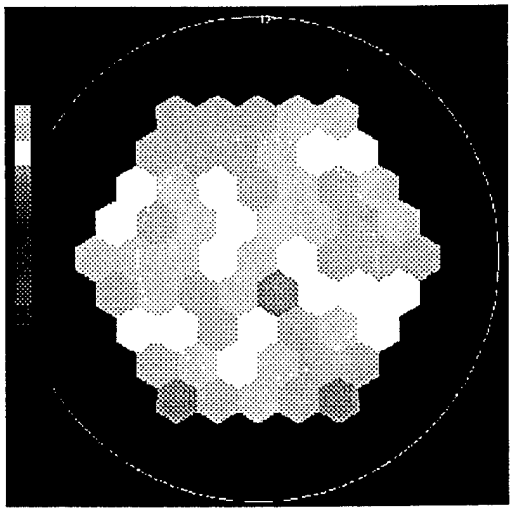

Fig. 4. The intensity coded 2-dimensional map calculated from the trace array in fig. 3..

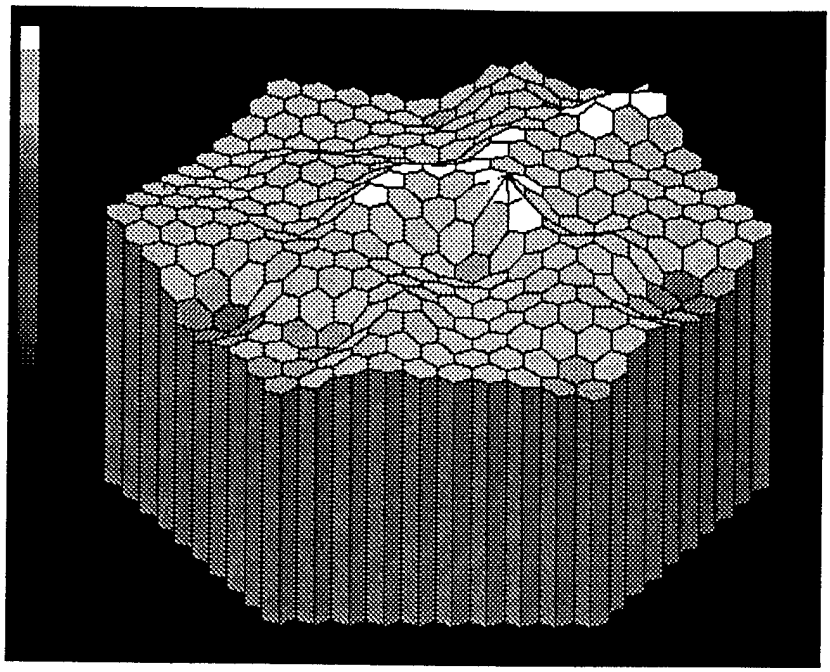

Fig. 5. Three dimensional topography of the trace array (scalar product) showing the volcano like shape of the central "hill of vision".

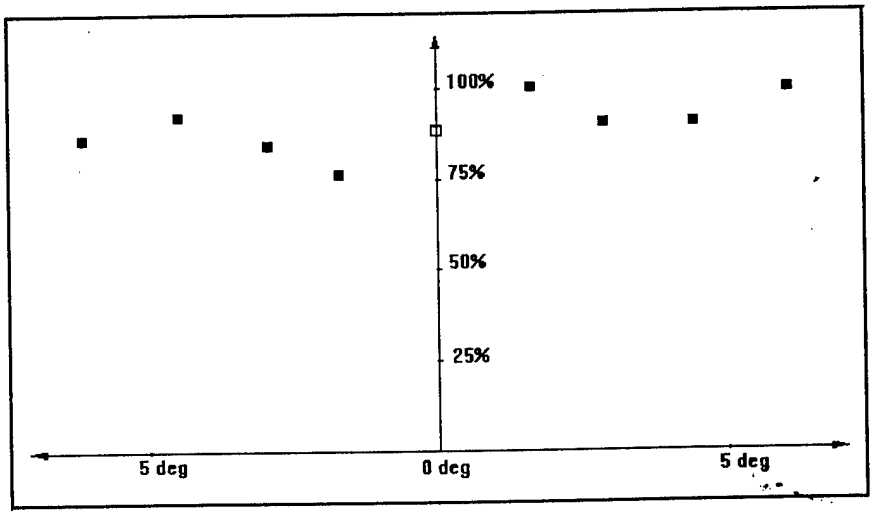

Fig. 6. Linear profile through the response minimum (i.e. the lesion).